doi:10.1006/jmbi.2001.4610 available online at http://www.idealibrary.com on IDEAL® *J. Mol. Biol.* (2001) **308**, 541–553

JMB

Conformational Spread in a Ring of Proteins: A Stochastic Approach to Allostery

T. A. J. Duke[1], N. Le Novère[2] and D. Bray[2]*

[1]*Cavendish Laboratory, Madingley Road, Cambridge CB3 0HE, UK*

[2]*Department of Zoology Downing Street, Cambridge CB3 3EK, UK*

**Corresponding author*

We recently suggested that the sensitivity and range of a cluster of membrane receptors in bacteria would be enhanced by cooperative interactions between neighbouring proteins. Here, we examine the consequences of this ''conformational spread'' mechanism for an idealised one-dimensional system comprising a closed ring of identical allosteric protomers (protein molecules, or a group of protein domains operating as a unit). We show analytically and by means of Monte Carlo simulations that a ring of allosteric protomers can exhibit a switch-like response to changes in ligand concentration. We derive expressions for the sensitivity and cooperativity of switching and show that the maximum sensitivity is proportional to the number of protomers in the ring. A ring of this kind can reproduce the sensitivity and kinetics of the switch complex of a bacterial flagellar motor, for example, which is based on a ring of 34 FliM proteins. We also compare smaller rings of conformationally coupled protomers to classical allosteric proteins such as haemoglobin and show that the canonical MWC and KNF models arise naturally as limiting cases. Conformational spread appears to be a natural extension of the familiar mechanism of allostery: a physically realistic mechanism that should apply widely to many structures built from protein molecules.

© 2001 Academic Press

Keywords: allostery; statistical mechanics; Monte Carlo simulation; flagellar motor

Introduction

The capacity of proteins to flip between two stable conformations in reversible fashion is a cornerstone of cellular physiology, and essential for such phenomena as cell signalling, cell movements, intermediary metabolism, and the selective expression of genes. Historically, our understanding of this fundamental molecular mechanism is based on studies of allosteric proteins, small oligomeric proteins such as haemoglobin whose conformation is affected by the binding of a small molecule. In haemoglobin and many hundreds of similar proteins, conformational changes take place in a symmetrically arranged oligomer of identical or closely similar proteins. The dihedral or rotational symmetry of such molecules increases the stability of their conformational states and enhances the abrupt, switch-like character of their transitions.[1] Analysis of haemoglobin and similar molecules led to algebraic formulations of great utility, notably that proposed by Monod, Wyman and Changeux (known as the MWC model)[2] and that proposed by Koshland, Némethy and Filmer (the KNF model).[3]

However, it is evident that conformational changes are not restricted to small symmetrical oligomers of a single type of protein. Many examples can be cited in which single asymmetric proteins change conformation in response to environmental stimuli, such as the binding of an ion or small molecule, chemical modifications, or exposure to temperature, light, pressure, and other physical agents. There are also situations in which proteins of one type influence the conformation of other proteins even when the two are unrelated in structure. This is how signals are thought to pass from transmembrane receptors to heterotrimeric G proteins, for example, and how the binding of calcium ions to troponin regulates the contraction of skeletal muscle. The recently described inhibitory influence of different transmitter-gated cation channels may depend on a similar mechanism.[4]

Furthermore, the classical view of allostery is limiting because it encourages us to think of the

Abbreviations used: MWC, Monod, Wyman and Changeux; KNF, Koshland, Nemethy and Filmer.

E-mail address of the corresponding author: d.bray@zoo.cam.ac.uk

0022-2836/01/030541–13 $35.00/0

© 2001 Academic Press

influence of one protomer on another as being deterministic or all-or-none, rather like the elements of a cellular automaton. However, the probability of such transitions which depends on the relative free energies of the two states, is a continuous variable that can change by a very small amount. Thus, it is possible that the conformational state of one protomer might cause only a marginal bias in favour of one conformation of a neighbouring protomer. A change of this kind, although small, could nevertheless have major physiological consequences.

In a recent analysis of the chemotactic signalling pathway of coliform bacteria, we suggested that the performance of a two-dimensional lattice of chemotactic receptors in the membrane of these organisms could be greatly enhanced if cooperative interactions occurred between adjacent proteins.[5] We showed, in a theory based on an analogous two-dimensional Ising model,[6] that the inclusion of a single free energy term due to cooperative interactions between adjacent receptors in the cluster could integrate the activities of receptors over the cluster. Selection of a suitable value for this interaction energy then led to a lowered threshold and a greatly increased range of detection. In the present study we have analysed the idea of conformational coupling further and applied it to the one-dimensional, unbounded case of proteins (or more generally protomers) in a closed ring. The simple geometry of this new situation allows us to define rigorously the conditions under which the ring will show cooperative switching. It also allows us to relate the physics of conformational spread to classical models of allostery.

Results

Ring model

We investigate the properties of an oligomer consisting of a closed ring of N identical protomers, which can be thought of as individual protein molecules, groups of proteins, or one or more protein domains that function as separate units. We wish, in particular, to include the possibility that ring protomers might be made up of domains from adjoining protein molecules, so that the interface between protomers is actually a flexible region within the protein structure. Each protomer in our formulation can exist in two distinct conformational states, which we designate active (+) and inactive (−), and makes rapid stochastic transitions between these states. A protomer may also bind a single molecule of an effector ligand, present in the surrounding solution at a concentration c. We assume that ligand binds the active site more strongly. In the absence of any other influences on the ring, thermodynamic considerations then dictate that the reciprocal condition is also true, namely that ligand binding shifts the conformational equilibrium and makes the active state more probable. For simplicity, we consider the symmetrical case in which the free energy of the active state, relative to that of the inactive state, changes from $+E_A$ to $-E_A$ when a protomer binds ligand (Figure 1(a)). Thermodynamic consistency then implies that the dissociation constant (K_d) of the ligand depends on the activity of the protomer according to:

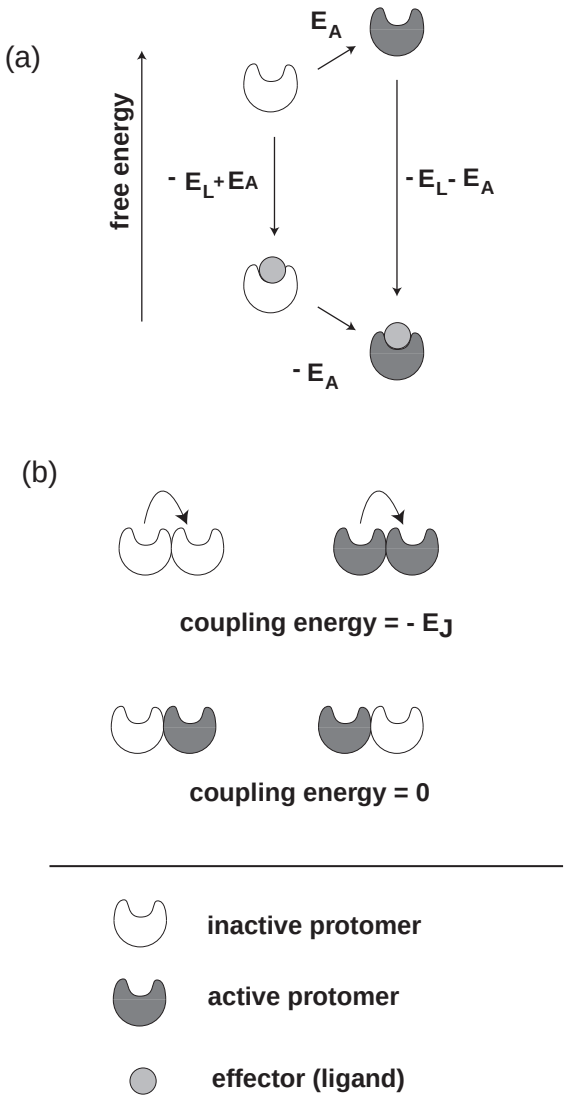

Figure 1. States of a ring protomer. Note that a ''protomer'' is here defined as a functional unit and is not necessarily an individual protein molecule; it could for example be two tightly bound domains belonging to adjacent proteins. (a) Each protein molecule, or protomer, in a ring can exist in an active conformation (black) or an inactive conformation (white) and may bind a single ligand molecule (grey). Transitions between inactive and active conformations are accompanied by a change of energy. Association with an effector molecule makes the active conformation more favourable energetically. Note that for simplicity we have considered a symmetric case in which the active → inactive transition involves a change in free energy of $+E_A$ in the absence of ligand, and $-E_A$ when ligand is bound. (b) Coupling energy. Conformation-dependent interactions between neighbouring protomers favour like conformations (or, equivalently, penalise opposite states).

$$K_d^+ \propto \exp\left(\frac{-E_L - E_A}{kT}\right), \quad K_d^- \propto \exp\left(\frac{-E_L + E_A}{kT}\right) \tag{1}$$

and

$$\frac{K_d^+}{K_d^-} = \exp\left(\frac{-2E_A}{kT}\right) \tag{2}$$

where K_d^+ and K_d^- are the dissociation constants of the ligand for active and inactive protomers, respectively, k is the Boltzmann constant and T the absolute temperature. E_L represents the ligand binding energy in the absence of conformational changes (that is, when $E_A = 0$). Crucially, we additionally suppose that there are conformation-dependent cooperative interactions between adjacent protomers that favour like conformational states. Again, we consider the symmetrical situation for simplicity and assume the free energy of a protomer to be reduced by E_J for each neighbouring protomer that is in the same conformational state (Figure 1(b)).

Performance of the ring

We carried out Monte Carlo simulations for protein rings of different sizes, built from protomers subject to the above energetic constraints. Each protomer can exist in one of 16 energy levels depending upon whether it is in an active or inactive conformation, whether or not it has a bound ligand, and whether its neighbouring protomers are in the active or inactive conformation (Table 1). The probability of a conformational transition of the protomer from state 1 to state 2 is proportional to $\exp(-(\text{energy}_2\text{-energy}_1)/kT)$. At each call of the simulation, the actual occurrence of a transformation is determined by comparing its probability with a random number, suitably scaled. The program visits protomers of the ring in a random sequence, at each call updating the energy and allowing a ligand molecule to bind or unbind according to the thermodynamically determined dissociation constants.

At any given concentration of the ligand, the activity of protomers in the ring fluctuates in time due to their individual stochastic flipping and the random binding and dissociation of ligand molecules. In the absence of coupling ($E_J = 0$) each protomer flips independently of its neighbours, generating a random pepper-and-salt pattern. But with the introduction of a non-zero coupling energy, E_J, conformational spread gives rise to contiguous regions, or domains, in which all protomers have the same state (Figure 2). Growth and shrinkage of domains occurs by a process analogous to diffusion and the domains become larger, on average, as the coupling strength increases. When the typical domain size exceeds the number of protomers in the ring, a coherent configuration is favoured. Then the ring spends the majority of the time in one or other of the two extreme configurations, in which all of the protomers have the same state (i.e. the ring is a single domain). In this situation, the ring behaves as a two-state switch. In general, it switches stochastically between the two extreme configurations, but the proportion of time spent in each configuration depends on the concentration of the effector ligand. The probability of the fully active configuration can increase sharply, from close to zero to almost unity, over a narrow range of effector concentration, making the switch

Table 1. Energy levels of a protomer

protomers	free energy		
	$-2E_J$		
	$-E_J$		
	$-E_J$		
	set to zero		
		$+E_A$	
	$-E_J$	$+E_A$	
	$-E_J$	$+E_A$	
	$-2E_J$	$+E_A$	
	$-2E_J$	$+E_A$	$-E_L$
	$-E_J$	$+E_A$	$-E_L$
	$-E_J$	$+E_A$	$-E_L$
		$+E_A$	$-E_L$
			$-E_L$
	$-E_J$		$-E_L$
	$-E_J$		$-E_L$
	$-2E_J$		$-E_L$

The free energy of each protomer in the ring is specified by its conformational state (whether active or inactive), the occupancy of its ligand-binding site, and the conformational states of its two nearest neighbours (see Figure 1 for an explanation of the symbols). Energy levels are those expected by the simplified assumptions stated in the text in which energy changes are symmetric with respect to ligand binding. Note also that we have here considered a structurally symmetric ring in which the clockwise neighbour has exactly the same influence as the counter-clockwise; the introduction of asymmetry does not alter our analysis.

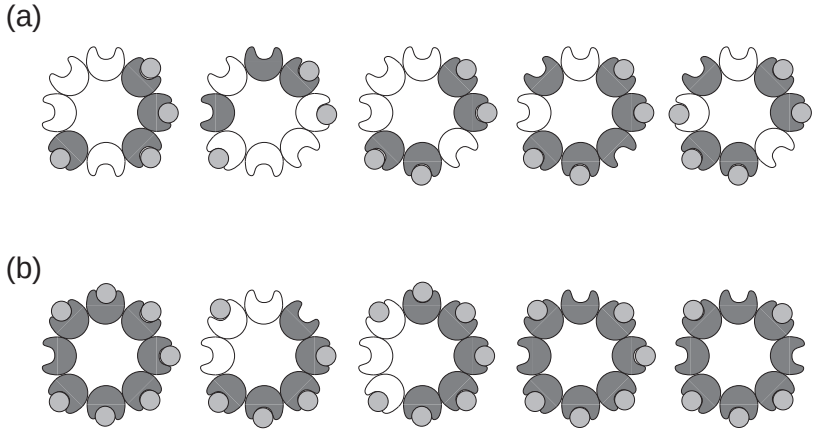

Figure 2. Typical changes in a protein ring. In this example, a ring of eight protomers was chosen and two sequential snapshots of its state are shown in the presence of a concentration $c_{0.5}$ of effector (a concentration leading to 50 % occupancy on average). In the first sequence (a) coupling is absent ($E_J = 0$) and the changes in protomers are uncoordinated; in the second (b) strong coupling ($E_J = 2kT$) results in coherent behaviour, with all of the protomers assuming the same state for most of the time.

extremely sensitive. Evidently, there is a critical coupling strength, E_J^*, above which switch-like behaviour ensues.

Switching

The critical coupling energy E_J^* for switching depends on the size of the ring. We define it by considering the situation in which non-extreme configurations of the ring are most likely to arise, which is when the mean occupancy is $\overline{Y}$=0.5. This corresponds to a ligand concentration $c \equiv c_{0.5} = \sqrt{K_d^+ K_d^-}$ (see Appendix). Our symmetry assumptions imply that the two coherent configurations of the ring (fully active or fully inactive), in which the ring is composed of a single domain, are equally probable in this case. Other configurations have alternating active and inactive domains around the ring such that the total number of domains is even. The probability of finding $2m$ domains, relative to the probability of each coherent configuration, is:

$$\frac{P(2m)}{P_{\text{coherent}}} = \binom{N}{2m} e^{-2mE_J/kT} \qquad (3)$$

where the first term is the number of ways of arranging the domains and the second term is the Boltzmann factor due to the energy associated with the domain walls. From this it can be seen that an extreme configuration is more probable than a configuration with two or more domains if:

$$E_J > E_J^* = kT \ln N, \quad (N \gg 1) \qquad (4)$$

This, then, is the condition under which a large ring has the character of a switch. We show below that the sensitivity of this switch (the sharpness of its transition) depends on other factors, notably the energy changes associated with ligand binding.

A more general version of this model would omit the assumption of symmetry. There would then be two separate energy differences between the active and inactive states: E_A^0 when a protomer is unliganded and E_A^1 when it is liganded. Also, there would be two different coupling energies: E_J^{--} between pairs of inactive protomers and E_J^{++} between active pairs (with the active-inactive interaction being taken as the reference). Together with $c_{0.5}$ (the concentration of ligand at which protomers of the ring are 50 % occupied on average, which is proportional to $\exp(-E_L/kT)$) this more general model would have five parameters.

Sensitivity of the switch

When equation (4) is satisfied, the protein ring operates as a switch controlled by the concentration of the diffusible ligand (the effector). At low concentrations, the switch is overwhelmingly in the fully inactive configuration. Occasionally, a single domain of active protomers is nucleated and, while this may fluctuate in size, it almost invariably vanishes after a brief interval of time. At higher ligand concentrations, approaching $c_{0.5}$, active domains are stabilised by the binding of ligand and can grow to encompass the whole ring. When this happens, the ring switches to the fully active configuration. In general, the ring is bistable at such intermediate concentrations and continually alternates between two coherent states. Note that even when the concentration of ligand is constant, each switching event is accompanied by a change in the average ligand occupancy, owing to the different affinities of the active and inactive protomers. At still higher concentrations of ligand, the switch assumes overwhelmingly the fully active configuration.

The dependability of the switch is determined by the narrowness of the bistable region: if the switch is very sensitive, it can be reliably turned ''on'' or ''off'' by moderate changes in ligand con-

centration. We define the sensitivity coefficient h_A as:

$$h_A \equiv \mathrm{Max}\left[\frac{d\ln(\bar{A}/(1-\bar{A}))}{d\ln(c/c_{0.5})\}}\right] \tag{5}$$

Where $\overline{A}$ is the mean activity of the ring. The calculation of $\overline{A}$ as a function of c in the Appendix leads to the result:

$$h_A \approx N\tanh\left(\frac{E_A}{2kT}\right)\left[\frac{6+(N-1)(N-2)e^{-2E_J/kT}}{6+3N(N-1)e^{-2E_J/kT}}\right], \quad E_J > E_J^* \tag{6}$$

In the limit of very strong coupling, the sensitivity becomes:

$$h_A(E_J \to \infty) = N\tanh\left(\frac{E_A}{2kT}\right) \tag{7}$$

and is therefore N times greater than that of an isolated protomer; that is, the maximum sensitivity is proportional to the number of protomers in the ring. The cooperativity coefficient h_Y for ligand binding (equivalent to the Hill coefficient) is also readily calculated in this case:

$$h_Y(E_J \to \infty) = 1 + (N-1)\tanh^2\left(\frac{E_A}{2kT}\right) \tag{8}$$

Relation to classical allosteric models

In order to provide a description of allosteric effects in proteins containing a small number of interacting subunits (such as haemoglobin) Monod, Wyman and Changeux (MWC) and Koshland, Nemethy and Filmer (KNF) developed models that make contrasting simplifying assumptions.[2,3] The two models are limiting cases of a general scheme discussed by Eigen[7] and illustrated in Figure 3(a). They also emerge naturally from the principles of conformational spread as limiting conditions in which either the junctional energy E_J, or the activation energy E_A, are allowed to become very large.

The MWC model rests essentially on two propositions (1) An oligomer ring can exist in only two extreme configurations (that is, the conformational change is all-or-none). (2) The ligand affinities of these two configurations are different. The MWC model is thermodynamically equivalent to our more general model in the limit where the two coupling strengths are very large ($E_J \gg E_J^*$). Mixed configurations are then prohibited, owing to their high energy, and the ring makes concerted transitions between the two extreme configurations. The MWC model contains two main parameters: L is the ratio of fully inactive to fully active configurations in the

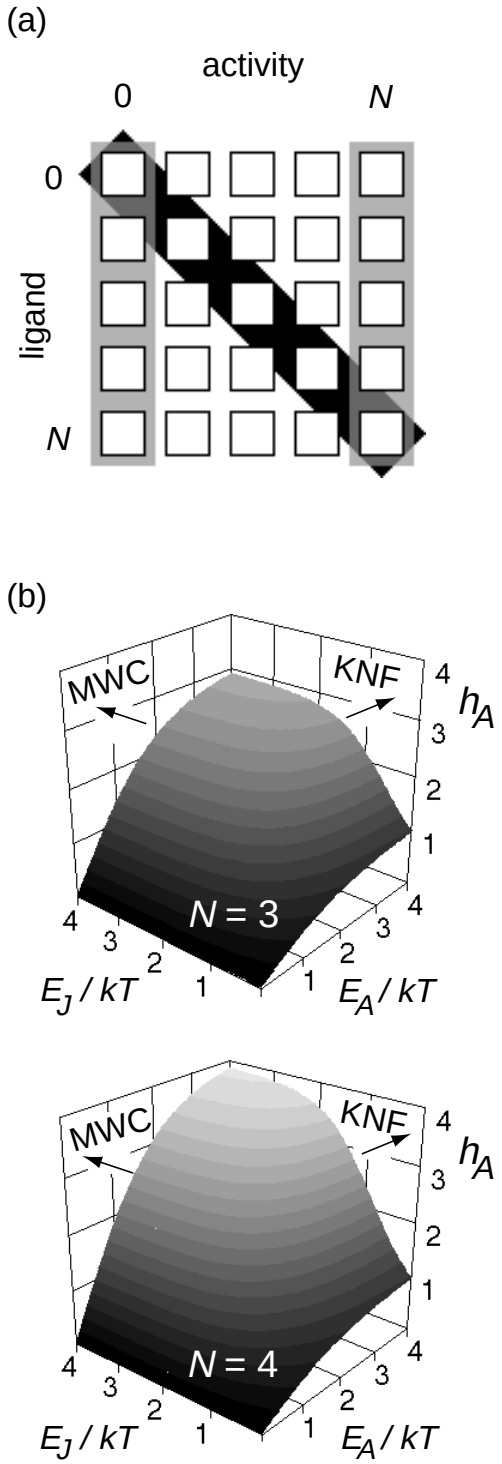

Figure 3. Allosteric models. (a) Permitted configurations of the oligomer ring in different models. Black, MWC concerted transition model; grey, KNF sequential model. The general scheme discussed in this article includes all possible configurations (in fact, there are more than are represented here, a total of 4^N). (b) Sensitivity coefficient h_A of rings of size $N = 3$ and $N = 4$ as a function of E_A and E_J. The limits $E_A \to \infty$ and $E_J \to \infty$ are equivalent to the KNF and MWC models, respectively.

absence of ligand (effector); and C is the ratio of the ligand affinities of the all-inactive and all-active configurations.[2] The MWC parameters are related to those of our general model as follows:

$$L = \exp\left(\frac{NE_A^0}{kT}\right), \quad C = \exp\left(\frac{E_A^0 + E_A^1}{kT}\right) \qquad (9)$$

It is of interest to note that the symmetric situation $E_A^0 = -E_A^1$ that we assumed above implies that $L = C^{-N/2}$. In this case, the MWC model reproduces equations (7) and (8) and the value of L is that which maximises the cooperativity h_Y and the sensitivity h_A, for a given value of C.[8] The symmetric case is consequently the most advantageous for creating a molecular switch (in this idealised situation of an isolated ring with only a single effector).

The KNF sequential model makes a quite different set of assumptions. (1) Each protomer is invariably inactive in the absence of ligand, but is forced to change conformation to the active state when the effector binds. (2) There are conformation-dependent cooperative interactions between neighbouring protomers. Since binding is always associated with conformational change, the cooperative interactions ensure that the effective affinity of the oligomer changes as successive effector molecules bind. Moreover, because the binding constants may be incorporated into the interaction energies, the KNF model may be described by just two parameters (in addition to $c_{0.5}$). These two parameters characterise the active-active and inactive-inactive interactions, with the active-inactive interactions taken as the reference. Thus, it can be seen that the KNF model is equivalent to our general model in the limit where the values of E_A^0 and $-E_A^1$ (free energy changes of activation in the absence or presence of ligand) both tend to infinity (see Figure 3(b)).

It is well known that some allosteric enzymes are more accurately described by the MWC model, while for others the KNF model provides the better picture. The general five-parameter version of our model provides a comprehensive description of allosteric effects in oligomer rings of arbitrary size and encompasses both classic models as limiting cases. The more restricted symmetric case considered in this paper, which involves just three parameters (E_A and E_J and $c_{0.5}$), is illuminating because it permits explicit analytic results, such as equation (6) to be obtained. Moreover, it highlights the separate contributions made by ligand binding and cooperative interactions to the sensitivity of the ring as a switch. The sensitivity may be written:

$$h_A = N \tanh\left(\frac{E_A}{kT}\right) f\left(\frac{E_J}{kT},\ N\right) \qquad (10)$$

where f is a function which increases abruptly from $1/N$ to unity in the vicinity of $E_J = E_J^*$. Thus, good sensitivity requires $E_A > kT$ and $E_J > E_J^*$.

For the symmetric case, we can calculate exactly the sensitivity of the two smallest rings, $N = 3$ and $N = 4$ as:

$$h_A(3) = 3 \tanh\left(\frac{E_A}{2kT}\right)\left[\frac{3 + e^{-2E_J/kT}}{3 + 9e^{-2E_J/kT}}\right] \qquad (11)$$

$$h_A(4) = 4 \tanh\left(\frac{E_A}{2kT}\right)\left[\frac{1 + e^{-2E_J/kT}}{1 + 6e^{-2E_J/kT} + e^{-4E_J/kT}}\right] \qquad (12)$$

from which we see that this model segues smoothly between the limiting cases represented by the MWC and KNF models (Figure 3).

Kinetics of switching

Since our model includes all possible configurations of the ring, it allows us to examine the kinetics of switching. This is particularly important for large rings, for which the concerted transitions implicit in the MWC model are unrealistic. Indeed, as a result of the different dissociation constants of the fully active and fully inactive configuration, an abrupt, concerted switch would cause the ring to have a non-equilibrium amount of ligand bound. It would therefore involve an activation energy that grows linearly with N, and so would become increasingly improbable for large rings. In our model, by contrast, a switch occurs by the accumulation of individual protomer transitions, which are stabilized by the binding or dissociation of ligand. The model requires just two fundamental kinetic parameters: the transition frequency ω at which a protomer makes a conformational transition and the rate k_{ligand} at which an effector molecule binds when $c = c_{0.5}$.

As we have already mentioned, a ring acts as a two-state switch if $E_J > E_J^*$. Then the sensitivity of the switch to the concentration of ligand depends on the value of the activation energy E_A. When $E_A = 0$, the ring switches spontaneously between the two extreme configurations, independently of the ligand concentration. The kinetics of this special case is simple to analyse, permitting us to establish an upper bound for the frequency at which the ring can switch between the two coherent configurations.

A switch from the fully inactive to the fully active configuration can be divided into two steps. First, a single protomer must undergo a conformational change, thereby nucleating an active domain. Since this nucleation event may occur at any location and involves the creation of two domain walls (energy change $+2E_J$), the rate at which it occurs is $k_{nucl} = N\omega \exp(-2E_J/kT)$. Secondly, the active domain must grow to encompass the whole ring, without disappearing. Since no energy changes are involved in the movement of a domain wall, the domain grows and shrinks by simple diffusion. The probability that it grows from size 1 to size N, without shrinking to zero, can be calculated by standard methods[9] to be

$p_{\text{grow}} = 1/N$. Thus, the overall rate of switching between the two extreme configurations may be estimated as:

$$k_{\text{switch}} = k_{\text{nucl}} p_{\text{grow}} = \omega e^{-2E_J/kT} \tag{13}$$

(in making this estimate, we have used the fact that the time spent during switching is negligible compared to the time spent between switches, which is a consequence of the condition $E_J > E_J^*$). Thus, the switching time increases as the coupling strength increases. Bearing in mind that the critical coupling strength depends on the size of the ring, equation (4), we conclude that the maximal rate at which a ring can switch between two bistable configurations also depends on its size:

$$k_{\text{switch}} < \frac{\omega}{N^2} \tag{14}$$

When E_A is non-zero, the state of the switch is influenced by the concentration of ligand. For a narrow range of concentrations close to $c_{0.5}$ the ring is bistable and switches spontaneously between the two extreme configurations. If ligand binding is much slower than the rate of conformational transitions ($k_{\text{ligand}} \ll \omega$), the overall switch rate can be considerably lower than the aforementioned maximal rate. This is a consequence of the different binding constants for active and inactive protomers: an active domain which gets nucleated by chance will remain energetically disfavoured until is it stabilised by the binding of ligand. Consequently, the initial growth of a domain is sub-diffusive and the probability of its disappearance is augmented. As a result, the switch frequency falls sharply as the value of E_A increases. This complex kinetics will be examined in more detail in a future publication.

The most effective switches are those that combine good sensitivity with a rapid kinetics. Sensitivity is greatest when E_A is considerably higher than the thermal energy kT, and E_J exceeds E_J^* by a fair margin (equation (6)). On the other hand, high values of E_A and E_J slow down the kinetics and thereby enhance the noise associated with stochastic switching, which could reduce the reliability of the switch. Optimal performance is obtained when $E_A \approx kT$ and $E_J \approx E_J^*$.

The model also indicates the time scale of fluctuations in the activity that arise in between switching events, while the ring is ostensibly in one of the bistable configurations. Small fluctuations away from the coherent configuration arise whenever a domain of the opposite state is nucleated, but fails to grow to encompass the whole ring. The typical duration, τ_{fluc}, of such a fluctuation may be calculated from the theory of mean first-passage times[9] (it is the average time taken for a domain of size 1 to shrink to size zero). The derivation is straightforward in the case $E_A = 0$, considered above, and leads to $\tau_{\text{fluc}} = 2N/3\omega$. Comparison with equation (14) indicates that the time scale of fluctuations is shorter than the typical time between switches by a factor of N, at least.

Illustrative case: the flagellar motor

A ring of proteins that probably acts a switch is found in the rotary motors by which bacteria such as *Escherichia coli* drive their flagella. Each of the six or so motors on the surface of an *E. coli* cell is a roughly cylindrical structure about 50 nm in diameter (Figure 4). The motors rotate at more than 100 revolutions per second (typically 300 rps for *E. coli* in an unloaded condition) and can abruptly reverse their direction of rotation on the scale of milliseconds.[10–12] Each motor is built from 40 or so different kinds of protein, several of which form rings around the cylindrical structure. One of these, designated C for cytoplasmic, contains about 34 copies of the protein FliM[13] and is thought to control switching of the motor between clockwise and counterclockwise rotation. Switching is controlled by the cytosolic concentration of the small diffusible protein CheYp, which binds in a 1:1 fashion to FliM.

In a wild-type bacterium without stimulation, the cytosolic concentration of CheYp is around 3 μM and the flagellar motors show stochastic reversals of rotation every second or so.[14] Even a small change in CheYp concentration up or down is sufficient to disrupt this pattern and produce a marked shift toward either clockwise or counterclockwise rotation. Recent experiments indicate a sensitivity coefficient of around 10, between CheYp concentration and rotational ''bias'' (the proportion of time spent in a counterclockwise direction).[15]

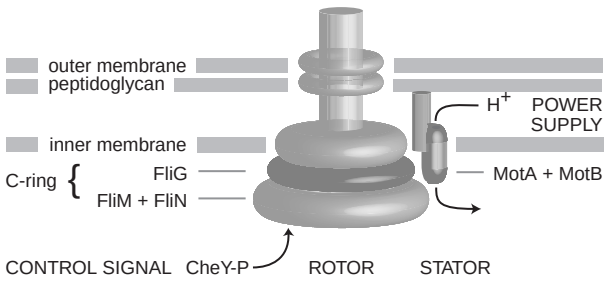

Figure 4. Flagellar motor. A cylindrical rod forms the central part, or ''drive shaft'' of the flagellar motor, passing through two hollow rings of protein embedded in the outer membrane. The hollow rings probably work like bearings and are not essential for force production (they are absent in some species of bacteria). The lower part of the central rod is associated with a circular complex of proteins, the C ring. The outer face of the C-ring is believed to interact with a stud-like ring of proteins called MotA and MotB, embedded in the plasma membrane (only one pair shown), to contribute directly to torque production. The inner face is built from about 34 copies of the protein FliM, each of which can interact with the cytoplasmic molecule CheYp. High concentrations of CheYp cause the motor to switch to a clockwise direction.

The molecular mechanism of the switch is unknown and the subject of some speculation.[16–18] However, it is widely believed that binding of CheYp molecules to individual FliM molecules of the C ring causes a change in their conformation, and that this in some way provokes the change in direction of rotation. In two recent studies, motor switching was interpreted by models in which binding of CheYp to the motor shifts the difference in free energy between the *cw* and *ccw* states.[19,20]

We used Monte Carlo methods to simulate the properties of an oligomer ring containing $N = 34$ protomers. The intrinsic flipping frequency of an individual protomer was set at $\omega = 10^4\ s^{-1}$, a plausible rate of protein conformational change (Na channels activate and deactivate in 0.1 to 1 ms; haemoglobin changes from the oxy to the deoxy-conformation in 20 μs).[21] The rate of ligand binding at $c = c_{0.5}$ was chosen to be $k_{ligand} = 10\ s^{-1}$. This rate is based on a typical rate of diffusion-limited binding for an uncharged protein of $3 \times 10^6\ M^{-1}\ s^{-1}$,[22,23] and the observation that the motor bias is 0.5 when the concentration of CheYp is 3 μM.[15] This implies that $c_{0.5} = 3\ \mu M$, since we have assumed a symmetric model. The energy difference between active and inactive conformations was set at $E_A = kT$, for reasons mentioned above, and the behaviour of the ring was studied as the coupling strength was varied. In the following discussion, we equate the active state of a protomer with *ccw* force production and the inactive state with *cw* force production. The average activity of the ring is equated to the rotational bias.

Figure 5(a) shows the behaviour of a ring of 34 FliM molecules exposed to a constant concentration of 3 μM CheYp (the concentration at which half of the FliM molecules are occupied, on average). Each time course is built up from a series of vertical records, or snapshots, taken at intervals of 50 ms. Each snapshot is made up of 34 pixels representing the 34 protomers of the ring, which are coloured to represent either the activity of the protomer or the presence of a bound CheYp molecule. When $E_J = 0$ (no coupling), the activity undergoes Gaussian fluctuations about a bias of 0.5. As the coupling strength increases, the magnitude of these fluctuations grows rapidly and their distribution becomes non-Gaussian. When E_J approaches the critical coupling strength E_J^* (which, from equation (4) is $E_J^* \approx 3.5\ kT$), the two extreme rotational biases, 0.0 (*cw* rotation) and 1.0 (*ccw* rotation) become significantly populated. Finally, when $E_J > E_J^*$, the ring spends most of the time in one or other rotational state and switches stochastically between them.

Each switching event is accompanied by a significant alteration in ligand occupancy. The sensitivity of the ring to CheYp concentration is demonstrated in Figure 5(b) and (c). A small (15 %) change in CheYp concentration causes a negligible effect in an uncoupled system. But in a coupled system, where $E_J > E_J^*$, it causes a large shift in the proportion of time that the ring spends in the fully-*ccw* configuration.

The rotational bias of the ring and its mean occupancy $\overline{Y}$ are plotted as a function of CheYp concentration c in Figure 6 for values of E_J on either side of E_J^*. There is a narrow range of concentrations in which $\overline{Y}$ shifts between the two binding curves that correspond to K_d^+ and K_d^-; this delimits the region of bistability in which the ring switches stochastically between the two extreme rotations. Because the proportion of time spent in the fully *ccw* configuration depends sensitively on c, the bias varies sharply over this range. The sensitivity coefficient is $h_A \approx 9$ when $E_J = 3\ kT$ and $h_A \approx 14$ when $E_J = 4\ kT$, in agreement with equation (6). Thus, the experimentally determined sensitivity,[15] $h_A = 10(\pm 1)$, is compatible with our model if $E_A \approx kT$ and $E_J \approx E_J^*$.

When E_J is larger than the critical coupling strength the ring switches rapidly from one extreme configuration to the other, and we can identify the times at which switching occurs with fair precision (Figure 7). We can also calculate the mean frequencies ($k_{cw \to ccw}$ and $k_{ccw \to cw}$) at which the motor switches between *cw* and *ccw* rotation. As shown in Figure 7 the typical switch frequency is approximately $1\ s^{-1}$ when CheYp is close to 3 μM, so that our choice of kinetic parameters is compatible with the frequency of stochastic switching observed experimentally.[14] Note that this switch rate is approximately ten times slower than the maximal spontaneous frequency (equation (14) gives $k_{switch} < 10\ s^{-1}$); the moderate value of the activation energy, $E_A = kT$, provides good sensitivity without affecting the kinetics too adversely. When CheYp > 3μM , the rate of the $cw \to ccw$ transition increases and that of the $cw \to ccw$ transition decreases; the converse happens when CheYp falls below 3 μM. The form of the concentration dependence is consistent with experimental data.[17]

Superimposed on the overall switches of motor direction (when $E_J > E_J^*$) are small fluctuations in the total number of *cw* protomers, which occur on a shorter time scale of about 10 ms (Figure 5(a), bottom panel). This duration is consistent with the theoretical discussion of τ_{fluc} in the preceding section. Such fluctuations are in accord with the small, rapid variations in rotation rate observed experimentally.[11,12] Rarer large fluctuations, which necessarily have longer duration (apparent in Figure 5(b), bottom panel), might be interpreted as occasional brief pauses in rotation.[12]

Discussion

In this study, we used statistical mechanics to show that conformational spread is a plausible mechanism, a logical and physically rigorous extension of known molecular properties. Many if not most protein molecules exist in at least two distinct conformations and switch from one to the

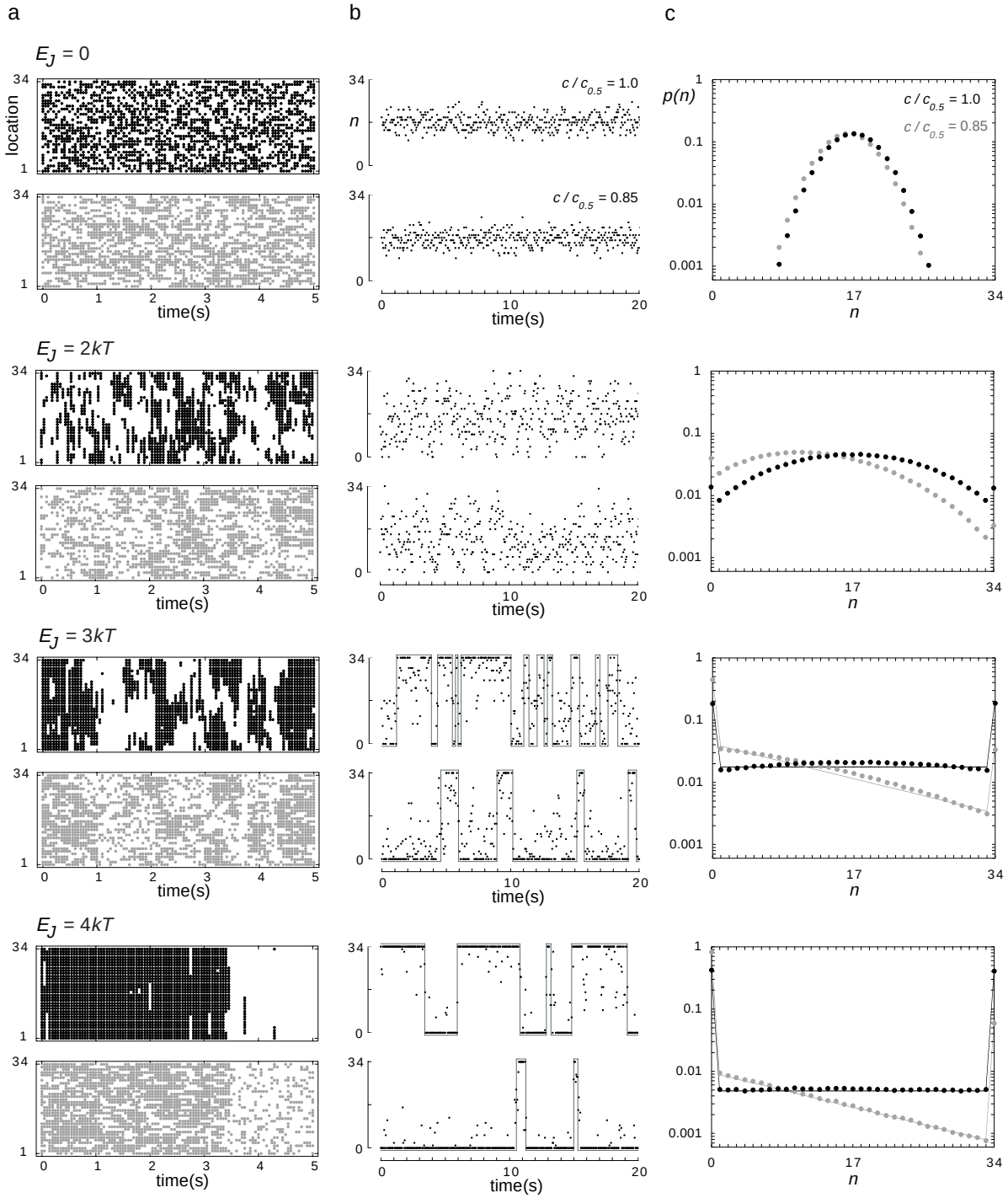

Figure 5. Predicted behaviour of the C-ring of the bacterial flagellar motor. The ring of 34 molecules of the protein FliM is analysed at four different values of the coupling energy, E_J (as noted in the text, the critical coupling energy $E_J^* \approx 3.5kT$). (a) Configuration of the ring as a function of time, the concentration of the effector molecule CheYp here being 3 μM (that is, $c = c_{0.5}$). Each block represents a series of vertical snapshots of the ring taken at intervals of 0.05 second, each pixel within a snapshot represents one of the 34 protomers. Black pixels represent active (*ccw*) protomers; grey pixels indicate the location of a bound CheYp molecule. Note that *ccw* protomers form a contiguous domain when $E_J > E_J^*$. (b) Number of *ccw* protomers (n) as a function of time for two different CheYp concentrations, 3 μM ($c = c_{0.5}$, upper trace) and 2.5 μM ($c = 0.85\ c_{0.5}$, lower trace). A clear switch-like character (indicated in grey) is evident when $E_J > E_J^*$. (c) Probability $p(n)$ that n protomers are in the *ccw* conformation for $c = c_{0.5}$ (black) and $c = 0.85\ c_{0.5}$ (grey). Lines are the analytical result given by equations (A6) to (A8), which is a good approximation when $E_J > E_J^*$.

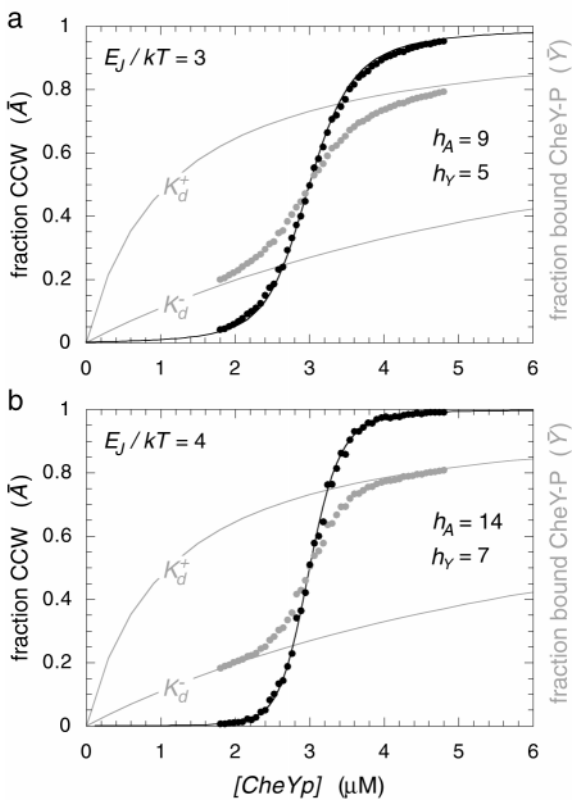

Figure 6. Response of the bacterial C-ring to the intracellular effector CheYp. The mean proportion of *ccw* protomers ($\bar{A}$, or the rotational bias) and the fraction of FliM protomers occupied by CheYp ($\bar{Y}$) are shown as functions of CheYp concentration, for two values of the coupling energy, E_J, both close to the critical value ($E_J^* \approx 3.5kT$). Grey lines represent the binding curves corresponding to binding constants K_d^- and K_d^+. Black lines are the value of $\bar{A}$ given by equation (A9), which is a good approximation when $E_J > E_J^*$. Values of the sensitivity coefficient h_A, estimated from the simulation data are marked; likewise, the values of the cooperativity coefficient for ligand binding h_Y. Note that the intersection of the two curves at the maximal slope is a consequence of the symmetrical model. In our generalised model the maximal slopes can occur at different ligand concentrations.

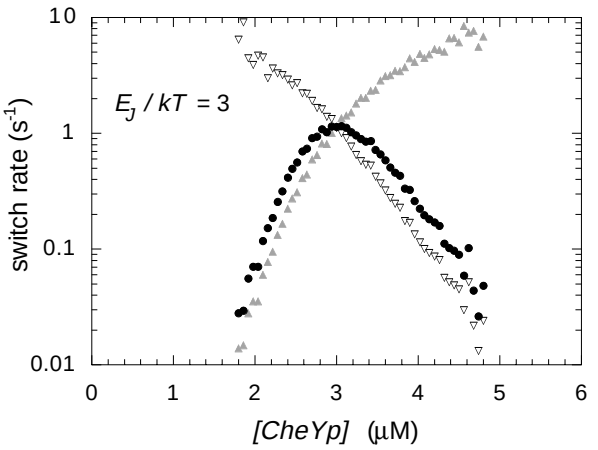

Figure 7. Kinetics of switching of the bacterial C-ring for a value of E_J close to the critical value. The average frequencies of transition between extreme conformations, $k_{cw \to ccw}$ (△) and $k_{ccw \to cw}$ (▽), are plotted as a function of the cytoplasmic concentration of CheYp, the effector molecule. Also shown is the total number of switches per second (●).

other in reversible fashion. Conformational changes can be induced by a wide variety of environmental stimuli such as physical effects and contact with other molecules. In a restricted set of allosteric proteins, it has been established that the conformations of individual subunits change in a coordinated, all-or-none fashion, often triggered by the binding of an effector molecule, or ligand. Our primary purpose in this study was to generalise from this behaviour of allosteric proteins to interactions that are graded rather than all-or-none, and to dissect out the different contributions to the free energy changes.

For ease of computation, we considered the idealised and computationally tractable case of a closed ring of identical subunits. Each protomer in the ring was assigned a free energy term that depended on the presence of a bound ligand, its own conformational state, the conformational state of neighbouring protomers and the strength of coupling between the two. The latter term was crucially important for the collective properties of the ring, and the larger this energy the more coherent was the response of the ring to external stimuli. Beyond a threshold, which depended on the size of the ring, the protomers had a high probability of sharing the same conformation at any instant of time. In this case, only two of the many potential quaternary structures were significant. The ring switched stochastically between these two extreme configurations, passing rapidly through a succession of configurations consisting of one active and one inactive domain.

We noted in a previous study that conformational changes can be formally mapped onto a statistical-mechanical model of magnetism: the random-field Ising model[5,6]. In this mapping, active protomers are regarded as up spins, inactive receptors as down spins, and there is a local magnetic field which points up at sites where ligand is present and down where no ligand is present. There is also, in contrast to the usual case studied in magnetism, a positive feedback between the spin and the local probability distribution of the field. This feedback arises because, at a given ligand concentration, the probability of ligand occupancy depends on the activity of a protomer (as a result of the two different dissociation constants).

The analogy with magnetism is useful because it permits a rapid evaluation of the conditions under which switch-like behaviour can occur, a preponderance of either of the extreme configurations corresponding to the presence of an ordered magnetic phase. It is well known, however, that there can be no phase transition in the one-dimensional nearest-neighbour Ising model which could spontaneously generate this order (in contrast to the two-dimensional case). This result holds despite the spin-field coupling, but it applies only in the ''thermodynamic limit'', for an infinitely long chain of protomers. Indeed, an indefinitely large ring cannot act as a switch. But oligomer rings of importance in the cell have a finite size. When the coupling energy exceeds a critical value (which increases with the size of the ring), conformational spread can extend over the entire ring, which in this case acts as a switch.

As a concrete illustration of the principles involved, we considered the ring of FliM molecules in the bacterial flagellar motor. Although this ring is part of the motor structure and closely associated with other proteins, we made the simplifying assumption that it operates in isolation to control motor switching. We assigned realistic values of concentrations, binding constants and Gibbs free energies to the model and then examined its response to changes in CheYp molecules. We found that the simulated ring underwent concerted changes in response to a precisely defined range of concentrations of the cytoplasmic signalling molecule, CheYp, and with a sensitivity coefficient comparable to that determined experimentally. An encouraging feature of this simulation was that the ring switched its state (equivalent to the motor changing its direction of rotation) stochastically at intervals of the order of $1\ s^{-1}$, even though the characteristic flipping time assumed for individual protomers was very much faster ($10^4\ s^{-1}$). We believe that similar ability to parlay the rapid motions of individual proteins into larger transitions on a physiologically relevant time scale might be found widely in living cells.

The collective behaviour of rings with a small number of protomers resembles that of classical allosteric proteins. A symmetrical oligomer with four identical subunits, for example, is equivalent to the usual case considered in models of allostery in haemoglobin (even though the haemoglobin molecule is actually a pair of homologous dimers in dihedral arrangement). Our simulations of conformational spread in a ring with $N = 4$ encompass all of the states of conformation and ligand occupancy formally recognized in previous models of haemoglobin, including those of the matrix schema proposed by Eigen.

The concerted transition considered in the MWC model, the model most commonly applied to haemoglobin, emerges as a limiting case of conformational spread in which the coupling energy, E_J, is extremely large. A large value of E_J could arise because of the aforementioned dihedral symmetry, which serves to strengthen bonding between protomers of similar state. The compact globular shape of the protomers also makes independent transitions of portions of the monomer less likely. The assumption of a large value of E_J together with other simplifying assumptions makes it easy to calculate from first principles the familiar parameters of the MWC model, including C and L. The concept of a ''quaternary structure'' in which all subunits of a protein adopt a limited number of coherent states is also given a precise meaning by this analysis, as a special condition at the boundary of parameter space.

Although our primary objective was to examine the behaviour of an idealised ring of proteins with generic properties, we note that actual rings of protein molecules are found widely in living systems. Isolated rings of a single species of protein are relatively hard to find, but instances in which rings are part of a larger protein-based structure, as in the flagellar motor described above, are abundant.[1]

One common function of protein rings is to form a channel or pore in a membrane. Voltage-gated cation channels have four subunits (or domains) in a ring; neurotransmitter-gated-ion channels have three to six homologous subunits; the connexons of gap junctions are made from two identical rings of six connexin proteins, stacked on top of each other. The complement membrane attack complex and perforin both form rings of variable size while the nuclear pore is a large complex of proteins with 8-fold symmetry. Further afield, pathogenic bacteria such as *Salmonella* translocate virulence factors into mammalian host cells by means of a large pore of InvG proteins with internal diameter 7 nm and made of about 12 subunits. In the bacterial flagellar motor, mentioned above, rings of proteins occur with $N = 8$, 10, 26 and 34.

Protein rings are also used for catalytic reasons, as with ATP synthase and CAM II kinase, or to enclose other molecules, as in the sliding clamps of DNA polymerase that form around a double helical DNA molecule. The large protein complexes of chaperones and proteasomes feature rings of seven identical subunits (and therefore have similar internal diameters). Larger rings include the 11 identical subunits in the Trp RNA-binding attenuation protein. The bacterial division protein FtsZ forms a ring-like structure with a diameter up to 0.5 μm and must contain several hundred subunits.

Any of these protein rings could, in principle, show allosteric interactions between their subunits and propagate changes in conformation. Some, indeed, are already known to undergo abrupt concerted switches in response to small changes in concentration of an effector molecule and therefore could act as control elements in the cell. Moreover, there is no reason why the notion of conformational spread should be restricted to a closed ring of identical subunits. For example, linear filaments could also act as switches although, at a fixed value of the

coupling energy, there would be a limit to the length of filament that could switch concertedly. As we have seen in this paper, conformational spread has the potential to integrate the dynamic behaviour of large numbers of protein molecules and to tune their collective performance to meet a variety of physiological requirements. It would be surprising if evolution had not taken advantage of this powerful mechanism.

Acknowledgements

We thank Jeremy Tame for helpful comments. This work was supported by a grant from the MRC (D.B) and a long term EMBO fellowship (N.L.N.).

References

1. Goodsell, D. S. & Olson, A. J. (2000). Structural symmetry and protein function. *Annu. Rev. Biophys. Biomol. Struct.* **29**, 105-153.
2. Monod, J., Wyman, J. & Changeux, J.-P. (1965). On the nature of allosteric transitions: a plausible model. *J. Mol. Biol.* **12**, 88-118.
3. Koshland, D. E., Némethy, G. & Filmer, D. (1966). Comparison of experimental binding data and theoretical models in proteins containing subunits. *Biochemistry,* **5**, 365-385.
4. Khakh, B. S., Zhou, X., Sydes, J., Galligan, J. J. & Lester, H. A. (2000). State-dependent cross-inhibition between transmitter-gated cation channels. *Nature,* **406**, 405-410.
5. Duke, T. A. J. & Bray, D. (1999). Heightened sensitivity of a lattice of membrane receptors. *Proc. Natl Acad. Sci. USA,* **96**, 10104-10108.
6. Shi, Y. & Duke, T. (1998). Cooperative model of bacterial sensing. *Phys. Rev. E,* **58**, 6399-6406.
7. Eigen, M. (1967). Kinetics of reaction control and information transfer in enzymes and nucleic acids. *Nobel Symp.* **5**, 333-369.
8. Rubin, M. M. & Changeux, J. P. (1966). On the nature of allosteric transitions: implications of non-exclusive ligand binding. *J. Mol. Biol.* **21**, 265-274.
9. Gardiner, C. W. (1996). *Handbook of Stochastic Methods*, 2nd edit., Springer Verlag, New York.
10. Berg, H. C. (1976). Does the flagellar rotary motor step? In *Cell Motility* (Goldman, R., Pollard, T. & Rosenbaum, J., eds), pp. 47-56, Cold Spring Harbor Laboratory Press, Cold Spring Harbor, NY.
11. Kudo, S., Magariyama, Y. & Aizawa, S. I. (1990). Abrupt changes in flagellar rotation observed by laser dark-field microscopy. *Nature,* **346**, 677-680.
12. Eisenbach, M., Wolf, A., Welch, M., Caplan, S. R., Lapidus, I. R., MacNab, R. M., Aloni, H. & Asher, O. (1989). Pausing, switching and speed fluctuations of the bacterial flagellar motor and their relation to motility and chemotaxis. *J. Mol. Biol.* **211**, 551-563.
13. Thomas, D. R., Morgan, D. G. & DeRosier, D. J. (1999). Rotational symmetry of the C ring and a mechanism for the flagellar rotary motor. *Proc. Natl Acad. Sci USA,* **96**, 10134-10139.
14. Block, S. M., Segall, J. E. & Berg, H. C. (1983). Adaptation kinetics in bacterial chemotaxis. *J. Bacteriol.* **154**, 312-323.
15. Cluzel, P., Surette, M. & Leibler, S. (2000). An ultrasensitive bacterial motor revealed by monitoring signaling proteins in single cells. *Science,* **287**, 1652-1657.
16. Berry, R. M. (1993). Torque and switching in the bacterial flagellar motor. An electrostatic model. *Biophys. J.* **64**, 961-973.
17. Turner, L., Caplan, S. R. & Berg, H. C. (1996). Temperature-induced switching of the bacterial flagellar motor. *Biophys. J.* **71**, 2227-2233.
18. Elston, T. & Oster, G. (1997). Protein turbines I: the bacterial flagllar motor. *Biophys. J.* **73**, 703-721.
19. Alon, U. C., Surette, M. G., Arcas, B. A., Liu, Y., Leibler, S. & Stock, J. B. (1998). Response regulator output in bacterial chemotaxis. *EMBO J.* **17**, 4238-4248.
20. Turner, L., Samuel, A. D. T., Stern, A. S. & Berg, H. C. (1999). Temperature dependence of switching of the bacterial flagellar motor by the protein $Che^{Y13DK106YW}$. *Biophys. J.* **77**, 597-603.
21. Hille, B. (1992). *Ionic Channels of Excitable Membranes*, 2nd edit., Sinauer Associates Inc, Sunderland, MA.
22. Camacho, C. J., Kimura, S. R., DeLisi, C. & Vajda, S. (2000). Kinetics of desolvation-mediated protein-protein binding. *Biophys. J.* **78**, 1094-1106.
23. Northrup, S. H. & Erickson, H. P. (1992). Kinetics of protein-protein association explained by Brownian dynamics computer simulation. *Proc. Natl Acad. Sci. USA,* **89**, 3338-3342.

Appendix

Activity *versus* concentration for an isolated protomer

In the following, we use 1 and 0 to represent liganded and unliganded protomers, and + and − to represent active and inactive conformations. From equation (1), the dissociation constants for the active and inactive states are, respectively, $K_d^+ = K_d \exp(-E_A/kT)$ and $K_d^- = K_d \exp(E_A/kT)$, where $K_d \propto \exp(E_L/kT)$. Thus, the product of the two constants is $K_d^+ K_d^- = K_d^2$. Now, K_d is the dissociation constant when $E_A = 0$ and so, in this case, half of the protomers are liganded when $c = K_d$. Our symmetry assumption implies that the average occupancy must remain equal to 0.5, at this concentration, when E_A is non-zero. Thus, $c_{0.5} = K_d = \sqrt{K_d^+ K_d^-}$.

The probability that an isolated protomer is liganded therefore depends on its activity:

$$\pi(1|+) = \frac{c}{c + c_{0.5} e^{-E_A/kT}} \qquad \text{(A1)}$$

$$\pi(1|-) = \frac{c}{c + c_{0.5} e^{E_A/kT}} \qquad \text{(A2)}$$

At the same time, the probability that the protomer is in the active conformation depends on whether or not ligand is bound:

$$\pi(+|1) = \pi(-|0) = \frac{1}{1 + e^{-E_A/kT}} \qquad \text{(A3)}$$

The overall probabilities that a protomer is active,

$\pi(+)$, or liganded, $\pi(1)$, may be calculated from these conditional probabilities using Bayes' rule:

$$\pi(+) = \pi(1)\pi(+|1) + \pi(0)\pi(+|0) \tag{A4}$$

$$\pi(1) = \pi(+)\pi(1|+) + \pi(-)\pi(1|-) \tag{A5}$$

Combining equations (A1) to (A5), the ratio of probabilities of active and inactive states for an individual protomer is:

$$\lambda \equiv \frac{\pi(+)}{\pi(-)} = \frac{ce^{E_A/kT} + c_{0.5}}{c + c_{0.5}e^{E_A/kT}} \tag{A6}$$

Activity *versus* concentration for an oligomer ring

We proceed by calculating the probability $p(n)$ that n protomers in the ring are active. When equation (2) is satisfied, the ring is most likely to be found in one of the extreme configurations, with relative probabilities given by:

$$\frac{p(N)}{p(0)} = \lambda^N \tag{A7}$$

It will, however, stochastically switch between these two configurations by passing through intermediate configurations in which different numbers of protomers are active. In equation (3), $P(2) \gg P(4)$, $P(6), \ldots$ when $E_J > E_J^*$, so in the switch-like regime we may assume that all of the active protomers form a single contiguous domain at all times. Then:

$$\frac{p(n)}{p(0)} \approx \frac{P(2)}{P_{\text{coherent}}}\lambda^n = Ne^{-2E_J/kT}\lambda^n, \ (1 \leqslant n \leqslant N-1) \tag{A8}$$

From equations (A7) and (A8), the mean activity (per protomer) of the ring, $\bar{A} = \overline{n}/N = \Sigma np(n)/N$ is given by:

$$\bar{A} \approx \frac{(1-\lambda)^2\lambda^N + e^{-2E_J/kT}[(N-1)\lambda^{N+1} - N\lambda^N + \lambda]}{(1-\lambda)^2(1+\lambda^N) + e^{-2E_J/kT}(1-\lambda)(\lambda - \lambda^N)N}, \quad E_J > E_J^* \tag{A9}$$

Edited by J. Karn

(Received 3 January 2001; received in revised form 7 March 2001; accepted 9 March 2001)